

Speciation, thermodynamics and structure of Np(v) oxalate complexes in aqueous solution†

M. M. Maiwald,^{*a} M. Trumm,^b K. Dardenne,^b J. Rothe,^b A. Skerencak Frech^b and P. J. Panak^{a,b}

The speciation, thermodynamics and structure of the Np(v) (as the NpO_2^+ cation) complexes with oxalate (Ox^{2-}) are studied by different spectroscopic techniques. Near infrared absorption spectroscopy (Vis/NIR) is used to investigate complexation reactions as a function of the total ligand concentration ($[\text{Ox}^{2-}]_{\text{total}}$), ionic strength ($I_m = 0.5\text{--}4.0 \text{ mol kg}^{-1} \text{ Na}^+(\text{Cl}^-/\text{ClO}_4^-)$) and temperature ($T = 20\text{--}85 \text{ }^\circ\text{C}$) for determination of the complex stoichiometry and thermodynamic functions ($\log \beta_n^0(T)$, $\Delta_r H_n^0$, $\Delta_r S_n^0$). Besides the solvated NpO_2^+ ion, two NpO_2^+ oxalate species ($\text{NpO}_2(\text{Ox})_n^{1-2n}$; $n = 1, 2$) are identified. With increasing temperature a decrease of the molar fractions of the 1:1 – and 1:2 – complexes is observed. Application of the law of mass action yields the temperature dependent conditional stability constants $\log \beta'_n(T)$ at a given ionic strength which are extrapolated to IUPAC reference state conditions ($I_m = 0$) according to the specific ion interaction theory (SIT). The $\log \beta_n^0(T)$ values of both complex species ($\log \beta_1^0(25 \text{ }^\circ\text{C}) = 4.53 \pm 0.12$; $\log \beta_2^0(25 \text{ }^\circ\text{C}) = 6.22 \pm 0.24$) decrease with increasing temperature confirming an exothermic complexation reaction. The temperature dependence of the thermodynamic stability constants is described by the integrated van't Hoff equation yielding the standard reaction enthalpies ($\Delta_r H_1^0 = 1.3 \pm 0.7 \text{ kJ mol}^{-1}$; $\Delta_r H_2^0 = 8.7 \pm 1.4 \text{ kJ mol}^{-1}$) and entropies ($\Delta_r S_1^0 = 82 \pm 2 \text{ J mol}^{-1} \text{ K}^{-1}$; $\Delta_r S_2^0 = 90 \pm 5 \text{ J mol}^{-1} \text{ K}^{-1}$) for the complexation reactions. In addition, the sum of the specific binary ion-ion interaction coefficients $\Delta \epsilon_n^0(T)$ for the complexation reactions are obtained from SIT modelling as a function of the temperature. The structure of the complexes and the coordination mode of oxalate are investigated using EXAFS spectroscopy and quantum chemical calculations. The results show, that in case of both species $\text{NpO}_2(\text{Ox})^-$ and $\text{NpO}_2(\text{Ox})_2^{3-}$, chelate complexes with 5-membered rings are formed.

1 Introduction

Spent nuclear fuel consists of unspent uranium, fission products, plutonium, and the minor actinides (Np, Am) generated by neutron capture reactions in the reactor. Some of these nuclides have very long half-lives and will determine the long-term radiotoxicity of the nuclear waste. Due to this fact, the high-level radioactive waste has to be isolated efficiently from the living environment for very long time periods. Thus, the emplacement of the radioactive waste in deep geological formations is the worldwide most preferred disposal option.^{1–3} For the safety case of a nuclear waste repository different incident scenarios have to be considered. For instance, the intru-

sion of water might result in the dissolution of the waste matrix followed by a variety of (geo)chemical reactions (dissolution, sorption, complexation in the aqueous phase, *etc.*) strongly affecting the migration behaviour of the actinides at repository conditions.⁴ For a detailed description of the chemical behaviour of actinides in natural aquatic systems a comprehensive thermodynamic model based on standard-state stability constants ($\log \beta_n^0$), standard reaction enthalpies ($\Delta_r H_n^0$) and entropies ($\Delta_r S_n^0$) is required.

For the final storage of high-level nuclear waste different types of host rock formations (clays, salt rocks, and crystalline formations) are discussed.^{1,5–11} Depending on the type of the host rock, different chemical conditions prevail including the presence of organic or inorganic ligands which may affect the geochemical behaviour of the actinides. For example, low molecular weight organic compounds (LMWOC) like formate, acetate, propionate, and lactate as well as macromolecular organic compounds are abundant in clay rocks and different natural systems serving as potential complexation agents.^{12–19} Furthermore, organic polymers, in particular polycarboxylates, used as additives in commercial concrete are another source

^aRuprecht Karls Universität Heidelberg, Physikalisch Chemisches Institut, Im Neuenheimer Feld 253, D 69120 Heidelberg, Germany.

E mail: m.maiwald@pci.uni-heidelberg.de

^bKarlsruher Institut für Technologie (KIT), Institut für Nukleare Entsorgung (INE), D 76344 Eggenstein Leopoldshafen, Germany

of organic macromolecules.^{20–22} Due to their complex structure the identification of binding sites or specific structural characteristics affecting the complexation properties ($\log \beta_n^0$, $\Delta_r H_n^0$, $\Delta_r S_n^0$) of these macromolecules is difficult. Furthermore, the decomposition of these organic compounds will lead to the formation of various small carboxylic ligands. Thus, simple and defined carboxylic ligands (*e.g.* oxalate, malonate, succinate, salicylate, phthalate) are used as reference systems for the organic macromolecules and their degradation products to study the effect of defined structural properties of organic molecules on the complexation properties toward actinides.

The temperature in the near-field of a nuclear waste repository will be increased due to the radioactive decay of the high-level nuclear waste. For example, in clay rock formations temperatures up to 100 °C are expected in the first time-period of post closure.²³ Furthermore, the porewaters of the used host rocks exhibit ionic strength of $I > 0$.^{14,24–26} For example, in clay rock formations in Northern Germany ionic strengths up to $I < 3.5 \text{ mol L}^{-1}$ are present. It is known that the temperature and the ionic strength significantly affect the complexation properties of the actinides. Thus, these effects must be considered for an accurate description of the complexation properties of actinides with organic matter and the determination of reliable thermodynamic functions ($\log \beta_n^0$, $\Delta_r H_n^0$, $\Delta_r S_n^0$).

The actinides U–Am are redox sensitive metal ions and exist as multi valent ions within the thermodynamic stability field of water.^{18,27–30} The pentavalent actinides (An(v)) are the most soluble actinide ions and thus will show a high mobility in case of water intrusion. In the series of the An(v) ions (U(v)–Am(v)) the Np(v) ion is the thermodynamically most stable species in aqueous solution and thus is used as an analogue for other An(v). Furthermore, the Np(v) ion exhibits excellent spectroscopic properties allowing an easy access for the determination of thermodynamic data.

In the literature data on the complexation of Np(v) with oxalate (Ox^{2-}) are scarce. Different studies by solvent extraction or absorption spectroscopy report $\log \beta_{25^\circ\text{C}}^0(\text{NpO}_2(\text{Ox})^-)$ values between 3.84 and 4.40 and $\log \beta_{25^\circ\text{C}}^0(\text{NpO}_2(\text{Ox})_2^{3-})$ between 5.8 and 7.36. $\Delta_r H_n^0$ and $\Delta_r S_n^0$ values are missing.^{18,31–34} There is only one study by Tian *et al.* using absorption spectroscopy and micro calorimetry on the temperature dependence of the complex formation revealing conditional enthalpy and entropy values at $I_m(\text{NaClO}_4) = 1.05 \text{ mol kg}^{-1}$ ($\Delta_r H'(\text{NpO}_2(\text{Ox})^-) = -12.2 \pm 0.1 \text{ kJ mol}^{-1}$, $\Delta_r H'(\text{NpO}_2(\text{Ox})_2^{3-}) = -25.5 \pm 0.1 \text{ kJ mol}^{-1}$ and $\Delta_r S'(\text{NpO}_2(\text{Ox})^-) = 27.4 \pm 0.6 \text{ J mol}^{-1} \text{ K}^{-1}$, $\Delta_r S'(\text{NpO}_2(\text{Ox})_2^{3-}) = 33.7 \pm 0.9 \text{ J mol}^{-1} \text{ K}^{-1}$).³²

In the present work the complexation of Np(v) with oxalate is systematically studied by near-infrared (Vis/NIR) absorption spectroscopy as a function of the ligand concentration ($[\text{Ox}^{2-}]_{\text{total}}$), ionic strength I_m (NaCl, NaClO_4), and temperature ($T = 20\text{--}85 \text{ }^\circ\text{C}$) revealing thermodynamic data at IUPAC reference state conditions ($\log \beta_n^0$, $\Delta_r H_n^0$, $\Delta_r S_n^0$) at room temperature and at elevated temperatures. Furthermore, no structural data of the formed complexes and information on the coordination modes of Ox^{2-} toward Np(v) are available. Thus, extended X-ray absorption fine structure spectroscopy (EXAFS) and

quantum chemical calculations are applied to investigate the structure of the Np(v)– Ox^{2-} complexes on a molecular level.

2 Experimental

2.1 Sample preparation

All solutions were prepared on the molal concentration scale (mol per kg per H_2O , “*m*”) because this concentration scale is independent of changes in temperature or ionic strength. All chemicals were reagent grade or higher and purchased from Merck Millipore or Alfa Aesar. For sample preparation ultra-pure water (Milli-Q academic, Millipore, 18.3 M Ω cm) was used.

For speciation studies by absorption spectroscopy an initial Np(v) concentration of $2.5 \times 10^{-4} \text{ mol kg}^{-1}$ was used and adjusted by dilution of a $6.1 \times 10^{-2} \text{ mol kg}^{-1}$ ²³⁷Np(v) stock solution in $2.9 \times 10^{-3} \text{ mol kg}^{-1}$ HClO_4 provided by the Institute for Nuclear Waste Disposal at the Karlsruhe Institute of Technology (KIT).³⁵ The total proton concentration ($[\text{H}^+]_{\text{total}} = [\text{H}^+]_{\text{eq}} + [\text{HOx}^-]_{\text{eq}} + 2 \cdot [\text{H}_2\text{Ox}]_{\text{eq}}$) in the samples was adjusted between $1.6\text{--}2.1 \times 10^{-5} \text{ mol kg}^{-1}$ by addition of a standardized 0.01 mol kg^{-1} HClO_4 or HCl solution. Thus, a direct measurement of the pH in the samples is not necessary as all equilibrium conditions are calculated from the known total concentrations in solution (see section 3.1.2).

The complexation of Np(v) with oxalate was studied as a function of the total ligand concentration ($[\text{Ox}^{2-}]_{\text{total}} = 0\text{--}1.4 \times 10^{-2} \text{ mol kg}^{-1}$) and temperature ($T = 20\text{--}85 \text{ }^\circ\text{C}$) at a fixed ionic strength ($I_m = 1.0 \text{ mol kg}^{-1}$ NaClO_4) ($[\text{Ox}^{2-}]_{\text{total}} = [\text{Ox}^{2-}]_{\text{eq}} + [\text{HOx}^-]_{\text{eq}} + [\text{H}_2\text{Ox}]_{\text{eq}}$). Solid Na_2Ox is used for preparation of the titration solutions. The ionic strength in the titration solution is adjusted to $I_m = 1.0 \text{ mol kg}^{-1}$ by addition of aliquots of solid NaClO_4 .

The ionic strength dependence was studied at fixed ligand concentrations ($[\text{Ox}^{2-}]_{\text{total}} = 1.6 \times 10^{-4}$, 3.2×10^{-4} , and $5.3 \times 10^{-3} \text{ mol kg}^{-1}$) and various concentrations of the background electrolytes (NaClO_4 , NaCl). The concentration of NaClO_4 was increased by successive addition of aliquots of an aqueous 14.0 mol kg^{-1} NaClO_4 solution. The concentration of NaCl was increased by addition of solid NaCl to the samples. The total proton concentration of all titration solutions was kept constant at $2.1 \times 10^{-5} \text{ mol kg}^{-1}$ using a standardized 0.01 mol kg^{-1} HClO_4 or HCl solution. Details on the experimental conditions are given in the ESI.†

For EXAFS measurements a Np(v) concentration of $5.0 \times 10^{-3} \text{ mol kg}^{-1}$ and an oxalate concentration of 0.1 mol kg^{-1} at $I_m(\text{NaClO}_4) = 1 \text{ mol kg}^{-1}$ was used. All EXAFS measurements were performed as a function of the conditional pH value ($\text{pH}_c = -\log [\text{H}^+]_{\text{eq}}$). The pH_c was varied between 1.8 and 5.0 by addition of small aliquots of a 1.0 mol kg^{-1} HClO_4 (Merck KGaA, suprapure). The pH_c was measured with a combination pH electrode (Orion™ PerpHecT™ ROSS™), which was calibrated with pH reference buffer solutions (Merck, pH = 8.00, 5.00, 2.00). Details on the definition of pH_c are given in the literature.^{36,37} The sample volume was 200 μL . The Np(v) con-

centration in the samples and the species distribution was determined by Vis/NIR absorption spectroscopy before and after the EXAFS measurements to ensure that no redox processes occurred during irradiation of the samples.

All uncertainties of the stability constants $\log \beta$, enthalpy ΔH , entropy ΔS and SIT binary ion-ion interaction coefficient $\Delta \epsilon_{j,k}$ are given with a confidence level of 0.95.

2.2 Vis/NIR absorption spectroscopy

Vis/NIR absorption spectra of Np(v) were recorded in the temperature range of 20–85 °C using a Varian Cary 5G UV/Vis/NIR spectrophotometer. The sample holder was temperature controlled using a Lauda Eco E100 thermostatic system (temp. accuracy: ± 0.5 °C). The samples (quartz glass cuvettes, 1 cm path length, Hellma Analytics) were equilibrated for 15 minutes at each temperature in a custom-made copper sample holder placed on a heating plate with thermostatic control (VWR Collection VMS-C4 Advanced with IKA (JANKE & KUNKEL) PT 1000 temperature sensor; temp. accuracy: ± 0.5 °C) to ensure chemical equilibrium of the sample solutions before measurement. Both thermostatic setups are calibrated with a precision laboratory thermometer (Amrell GmbH & Co. KG, DIN 12775; temp. accuracy: ± 0.5 °C) to ensure that the temperature of the aqueous solution inside the cuvettes is correct. The spectra were recorded between 950–1050 nm with a data interval of 0.1 nm, a scan rate of 60 nm min⁻¹ (average accumulation time 0.1 s) and a slit width of 0.7 nm in double beam mode.

2.3 EXAFS measurements

Np-L₃-EXAFS spectra were measured in fluorescence mode at the INE-Beamline of the Karlsruhe Research Accelerator, KARA, at KIT.^{38–40} For recording of the fluorescence light a 4 element Si SDD Vortex (SIINT) fluorescence detector and a 1 element Si Vortex-60EX SDD (SIINT) fluorescence detector at an angle of 90° were used. The optical components of the beamline consisted of a double-crystal monochromator (DCM) with a Ge(422) crystal pair and a collimating and focusing mirror system (Rh-coated silicon mirrors). The DCM was detuned in the middle of the scan range to 70% peak flux intensity. An Ar-filled ionization chamber was used to measure the intensity I_0 of the incident X-ray beam. Within the EXAFS range, the measurements were performed at equidistant k -steps and an increasing integration time following a $\sqrt{2}$ progression. The data evaluation was performed with the software packages EXAFSPAK, Athena – Demeter 0.9.26, and Artemis – Ifeffit 0.8.012.^{41–43} The crystal structures of UO₂-oxalate were used for calculation of the theoretical scattering phases and amplitudes using FEFF8.40 and replacing U by Np.^{44–46} In all cases, the models were fitted to the k^2 - and k^3 -weighted raw EXAFS spectra.

2.4 Quantum chemical calculations

Structure optimizations of the Np(v) oxalate complexes were carried out on density functional theory (DFT) level using the TURBOMOLE 7.0 program package.⁴⁷ The BH-LYP functional was chosen for its better convergence compared to other

hybrid-functionals. All C, O and H atoms were represented by basis sets of triple zeta basis quality (def-TZVP) and were treated at the all-electron level.^{47,48} The metal ion was represented by a 60-electron core pseudo-potential (Np, ECP60MWB) with corresponding basis sets of triple-zeta quality.⁴⁹ The NpO₂(Ox)⁻ and NpO₂(Ox)₂³⁻ complexes with different coordination modes (end-on vs. side-on) of the ligand molecules were optimized. The gas phase energies E_g of the triplet ground states were computed on the MP2 level. Additionally, for a theoretical approximation of the Gibbs free energies (G) thermodynamic corrections ($E_{\text{vib}} = E_{\text{zp}} + H_0 - TS$, E_{zp} being the zero-point energy; H_0 and S are the enthalpy and entropy of the complexes obtained from calculations of the vibrational modes) and solvation energies E_{solv} (obtained using COSMO, $r_{\text{Np}} = 1.72$ Å) were taken into account. The Gibbs free energies were calculated as follows: $G = E_g + E_{\text{vib}} + E_{\text{solv}}$.^{50–52} Due to the ionic form of the Np(v) complexes a full second hydration shell was added and optimized to avoid the charge of the complexes to contact the COSMO cavity.

3 Results and discussion

3.1 Vis/NIR absorption spectroscopy

3.1.1 Absorption spectra. The absorption spectra of Np(v) with increasing total oxalate concentration $[\text{Ox}^{2-}]_{\text{total}}$ at 20 °C and $I_m(\text{NaClO}_4) = 1.0$ mol kg⁻¹ are displayed in Fig. 1. The absorption band of the Np(v) aquo ion is located at 980.1 ± 0.1 nm ($\epsilon_{\text{max}} = 396 \pm 4$ l mol⁻¹ cm⁻¹). With increasing $[\text{Ox}^{2-}]_{\text{total}}$ a bathochromic shift of the absorption band and the formation of two additional absorption maxima at about 988 nm and 995 nm are observed. Furthermore, two isosbestic points are located at 984.2 ± 0.2 and 990.9 ± 0.2 nm. At elevated temperatures similar observations are made but the bathochromic shift is less pronounced.

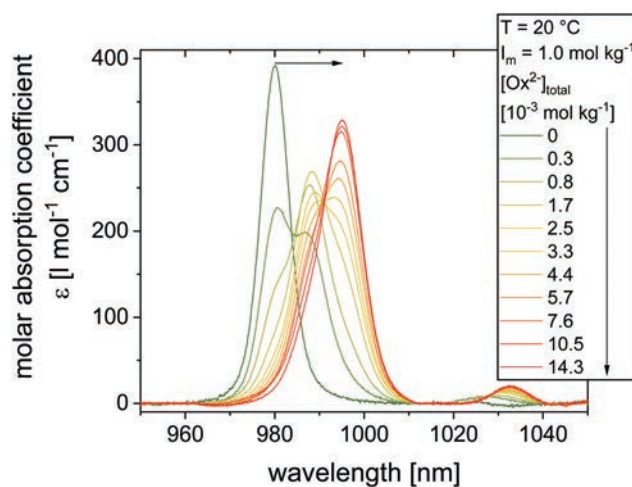


Fig. 1 Vis/NIR absorption spectra of the Np(v) ion with increasing total oxalate concentration. $[\text{Ox}^{2-}]_{\text{total}} = 0.0$ – 14.3×10^{-3} mol kg⁻¹ at $I_m(\text{NaClO}_4) = 1.0$ mol kg⁻¹; $T = 20$ °C; $[\text{H}^+]_{\text{total}} = 2.1 \times 10^{-5}$ mol kg⁻¹; $[\text{NpO}_2^+]_{\text{total}} = 2.5 \times 10^{-4}$ mol kg⁻¹.

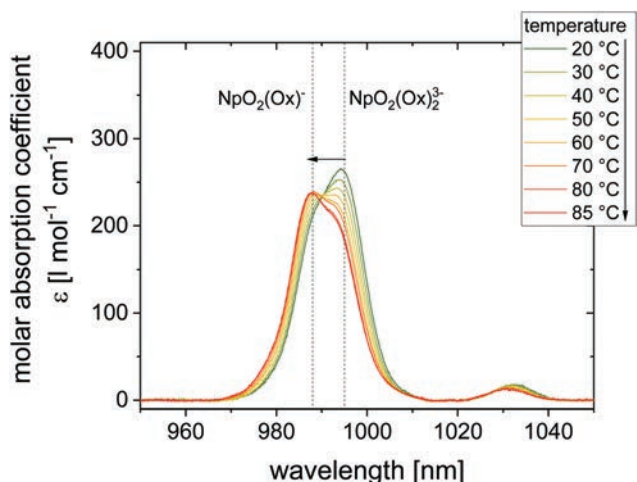


Fig. 2 Vis/NIR absorption spectra of the Np(v) ion as a function of the temperature at $[\text{Ox}^{2-}]_{\text{total}} = 4.4 \times 10^{-3} \text{ mol kg}^{-1}$ and $I_m(\text{NaClO}_4) = 1.0 \text{ mol kg}^{-1}$; $[\text{H}^+]_{\text{total}} = 2.1 \times 10^{-5} \text{ mol kg}^{-1}$; $[\text{NpO}_2^+]_{\text{total}} = 2.5 \times 10^{-4} \text{ mol kg}^{-1}$.

The temperature effect on the absorption spectra of Np(v) at a fixed oxalate concentration ($[\text{Ox}^{2-}]_{\text{total}} = 4.4 \times 10^{-3} \text{ mol kg}^{-1}$) is shown in Fig. 2. With increasing temperature a hypsochromic shift of the absorption band occurs indicating that the complexation of Np(v) with oxalate is repressed at elevated temperatures and confirming exothermic complexation reactions.

3.1.2 Peak deconvolution and speciation. The determination of the species distribution requires the single component spectra of the formed Np(v)–oxalate complexes. The spectra are derived *via* subtractive peak deconvolution using the spectrum of the Np(v) aquo ion. Details on this method are given in the literature.⁵³ Using this approach the absorption spectra of two different Np(v)–oxalate complexes are deconvoluted at all temperature and ionic strength conditions. The spectra at 20 and 85 °C and $I_m(\text{NaClO}_4) = 1.0 \text{ mol kg}^{-1}$ are displayed in Fig. 3. At 20 °C the absorption maximum of the first complex species $\text{NpO}_2(\text{Ox})^-$ is located at $987.8 \pm 0.1 \text{ nm}$ and is bathochromically shifted by 7.7 nm compared to the Np(v) aquo ion. The absorption band of $\text{NpO}_2(\text{Ox})_2^{3-}$ is located at $995.4 \pm 0.1 \text{ nm}$ corresponding to a bathochromic shift of 15.3 nm. Thus, a bathochromic shift of about 7.7 nm occurs for each coordinating oxalate molecule. At 85 °C the spectrum of the Np(v) aquo ion is hypsochromically shifted by 1.7 nm compared to 20 °C. The spectra of both Np(v)–oxalate complexes are shifted only by 1.3 nm in this temperature interval. Thus, the effect of the temperature on the absorption bands of the Np(v)–oxalate complexes is weaker compared to the Np(v) aquo ion. According to the literature, the hypsochromic shift of the Np(v) absorption was contributed to solvatochromic effects or changes of the solvation of the Np(v) ion in the first and second hydration shell.^{54–60} As the effect of temperature changes with the complexation of the Np(v) ion the composition of the first coordination sphere of the Np(v) ion seems to have a major impact on this temperature effect.

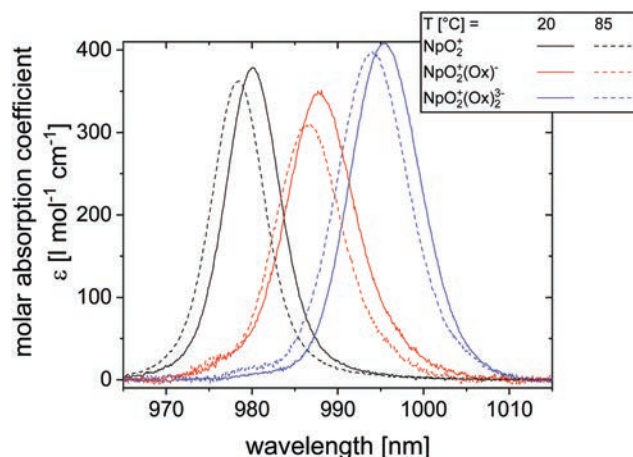


Fig. 3 Vis/NIR absorption spectra of the NpO_2^+ ion and the $\text{NpO}_2(\text{Ox})_n^{1-2n}$ ($n = 1, 2$) complexes at $T = 20$ (lines) and 85 °C (dashed lines) and $I_m(\text{NaClO}_4) = 1.0 \text{ mol kg}^{-1}$.

Furthermore, the observed hypsochromic shift of the absorption spectra of the Np(v)–oxalate complexes compared to the Np(v) aquo ion is in excellent agreement to that of other Np(v) complexes described in the literature. Yang *et al.* and Zhang *et al.* studied the complexation of Np(v) with benzoate and picolinate by absorption spectroscopy in a temperature range of 10–70 °C.^{61,62} In comparison to the hypsochromic shift of the Np(v) aquo ion of 1.8–1.9 nm the hypsochromic shifts of $\text{NpO}_2(\text{L})$ are 1.5 nm (L = picolinate) and 1.7 nm (L = benzoate). The spectrum of $\text{NpO}_2(\text{L})_2$ shifts by 1.6 nm (L = picolinate). In the literature this is explained by the more rigid Np(v)–ligand bond compared to the Np(v)–water bond resulting in a hindered thermal expansion of the metal–ligand bonds in the complexes compared to the Np(v) aquo ion. Nevertheless, the temperature induced hypsochromic shift of the absorption band of the Np(v) ion is contrary to the bathochromic shift resulting from the complexation reactions and requires the determination of single component spectra for all studied temperature conditions.

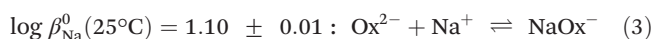
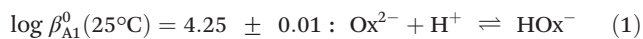
The spectroscopic characteristics of the Np(v)–oxalate complexes at 20 and 85 °C are summarized in Table 1

Deconvolution of the absorption spectra as a function of $[\text{Ox}^{2-}]_{\text{total}}$ by principle component analyses reveals the species distribution of the formed Np(v)–oxalate complexes as a function of the equilibrium concentration of oxalate $[\text{Ox}^{2-}]_{\text{eq}}$. An

Table 1 Spectroscopic properties of the absorptions spectra of the Np(v) aquo ion and $\text{NpO}_2(\text{Ox})_n^{1-2n}$ ($n = 1, 2$) at 20 and 85 °C and $I_m = 1.0 \text{ mol kg}^{-1} \text{ NaClO}_4$

T [°C]	Species	λ_{max} [nm]	ϵ_{max} [$\text{l mol}^{-1} \text{ cm}^{-1}$]	FWHM [nm]
20	NpO_2^+	980.1 ± 0.1	396 ± 4	7.4 ± 0.4
	$\text{NpO}_2(\text{Ox})^-$	987.8 ± 0.1	367 ± 16	9.4 ± 0.5
	$\text{NpO}_2(\text{Ox})_2^{3-}$	995.4 ± 0.1	426 ± 18	9.6 ± 0.5
85	NpO_2^+	978.4 ± 0.1	374 ± 10	7.3 ± 0.4
	$\text{NpO}_2(\text{Ox})^-$	986.5 ± 0.1	323 ± 13	9.2 ± 0.5
	$\text{NpO}_2(\text{Ox})_2^{3-}$	993.9 ± 0.1	414 ± 17	9.7 ± 0.5

exemplary deconvolution is given in the ESI in Fig. S1.† There is no indication for additional chemical species present others than the used ones. Four different chemical species of oxalate can exist in aqueous solution which are H_2Ox , HOx^- , Ox^{2-} and NaOx^- . Thus, the following chemical reactions have to be accounted for in the calculation of $[\text{Ox}^{2-}]_{\text{eq}}$:⁶³⁻⁶⁵



The calculations are performed with the software package Hyperquad Hyss2008, Version 4.0.31.⁶⁶ $[\text{Ox}^{2-}]_{\text{eq}}$ is determined as a function of $[\text{Ox}^{2-}]_{\text{total}}$, $[\text{H}^+]_{\text{total}}$, I_m and T .^{18,67} The temperature dependence of the protonation reaction of Ox^{2-} and the formation of NaOx^- is well described in the literature.⁶³⁻⁶⁵ Thus, $\log \beta_{\text{A}1}(T)$, $\log \beta_{\text{A}2}(T)$ and $\log \beta_{\text{Na}}(T)$ at a given temperature are calculated with the integrated van't Hoff equation using the thermodynamic data given in the literature ($\Delta_r H_{\text{A}1,m}^0 = 7.3 \pm 0.1 \text{ kJ mol}^{-1}$, $\Delta_r H_{\text{A}2,m}^0 = 10.6 \pm 0.6 \text{ kJ mol}^{-1}$, $\Delta_r H_{\text{Na},m}^0 = -5.0 \pm 0.7 \text{ kJ mol}^{-1}$). The ionic strength dependence is accounted for by application of the specific ion interaction theory (SIT). The required binary ion-ion interaction coefficients are given in the Nuclear Energy Agency Thermochemical Database (NEA-TDB) ($\epsilon(\text{Na}^+, \text{Cl}^-) = 0.03 \pm 0.01$, $\epsilon(\text{Na}^+, \text{ClO}_4^-) = 0.01 \pm 0.01$, $\epsilon(\text{H}^+, \text{Cl}^-) = 0.12 \pm 0.01$, $\epsilon(\text{H}^+, \text{ClO}_4^-) = 0.14 \pm 0.02$, $\epsilon(\text{Na}^+, \text{HOx}^-) = -0.07 \pm 0.01$, $\epsilon(\text{Na}^+, \text{Ox}^{2-}) = -0.08 \pm 0.01$, $\epsilon(\text{Na}^+, \text{NaOx}^-) \approx \epsilon(\text{Na}^+, \text{HOx}^-) = -0.07 \pm 0.01$).^{63,64,68}

In Fig. 4 the speciation (symbols) of the Np(v)-oxalate complexes is shown as a function of $[\text{Ox}^{2-}]_{\text{eq}}$ at 20 and 85 °C at $I_m = 1.0 \text{ mol kg}^{-1} \text{ NaClO}_4$. The calculated speciation (lines) using the derived $\log \beta'_n(T)$ values ($\log \beta'_1(20^\circ\text{C}) = 4.12 \pm 0.04$, $\log \beta'_2(20^\circ\text{C}) = 6.81 \pm 0.05$, $\log \beta'_1(85^\circ\text{C}) = 3.91 \pm 0.04$, $\log \beta'_2(85^\circ\text{C}) = 6.46 \pm 0.07$) is also displayed.

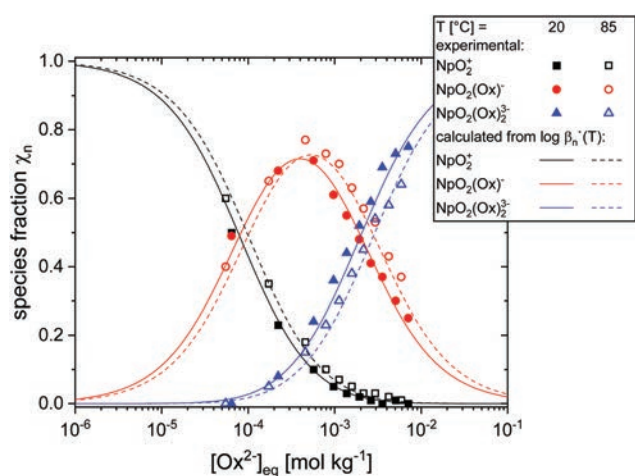
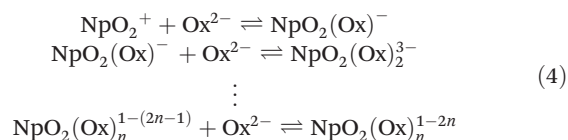


Fig. 4 Experimentally determined (symbols) and calculated species distribution of $\text{NpO}_2(\text{Ox})_n^{1-2n}$ ($n = 0, 1, 2$) complexes as a function of the equilibrium ligand concentration in aqueous solution. $I_m(\text{NaClO}_4) = 1.0 \text{ mol kg}^{-1}$; $T = 20^\circ\text{C}$ (solid lines) and 85°C (dashed lines).

With increasing $[\text{Ox}^{2-}]_{\text{eq}}$ the complexation equilibrium shifts toward the Np(v)-oxalate species. At 85 °C the species distribution is shifted toward the Np(v) aquo ion confirming exothermic complexation reactions.

3.1.3 Complex stoichiometry. The complex stoichiometry of the oxalate complexes is confirmed by slope analyses using the determined speciation at each studied temperature. The following complexation is applied:



According to the complexation model the slope analyses are performed using eqn (5):

$$\begin{aligned} \log K'_n &= \log \frac{[\text{NpO}_2(\text{Ox})_n]^{1-2n}}{[\text{NpO}_2(\text{Ox})_{n-1}]^{1-2(n-1)}} - 1 \times \log[\text{Ox}^{2-}]_{\text{eq}}; \\ \log \beta'_n &= \sum \log K_n \end{aligned} \quad (5)$$

Thus, slopes of $m = 1$ indicate that the species χ_n and χ_{n-1} differ by one coordinating oxalate molecule. Details on this procedure are given in the literature.⁶⁹⁻⁷¹

The slope analyses for 20 and 85 °C at $I_m = 1.0 \text{ mol kg}^{-1}$ are displayed in Fig. 5. The results show a linear correlation of $\log([\text{NpO}_2(\text{Ox})_n]^{1-2n}/[\text{NpO}_2(\text{Ox})_{n-1}]^{1-2(n-1)})$ with $\log([\text{Ox}^{2-}]_{\text{eq}})$. Linear regression analyses reveal slopes of 0.9 ± 0.1 to 1.0 ± 0.1 at all experimental conditions. Thus, the formation of two oxalate complexes with the stoichiometry of $\text{NpO}_2(\text{Ox})_n^{1-2n}$ and $n = 1, 2$ is confirmed.

3.1.4 Thermodynamic data. The determination of thermodynamic functions ($\log \beta'_n(T)$, $\Delta_r H_{m,n}^0$, $\Delta_r S_{m,n}^0$) at IUPAC reference state conditions ($I_m = 0$, $T = 298 \text{ K}$) requires conditional stability constants $\log \beta'_n(T)$ at various I_m and T . These data are extrapolated to $I_m = 0$ with the SIT according

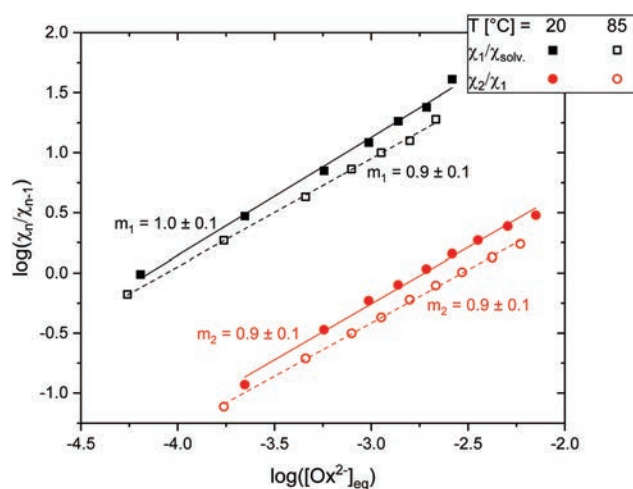


Fig. 5 Plots of $\log([\text{NpO}_2(\text{Ox})_n]^{1-2n}/[\text{NpO}_2(\text{Ox})_{n-1}]^{1-2(n-1)})$ vs. $\log([\text{Ox}^{2-}]_{\text{eq}})$ and linear regression analyses at $T = 20, 85^\circ\text{C}$ and $I_m(\text{NaClO}_4) = 1.0 \text{ mol kg}^{-1}$.

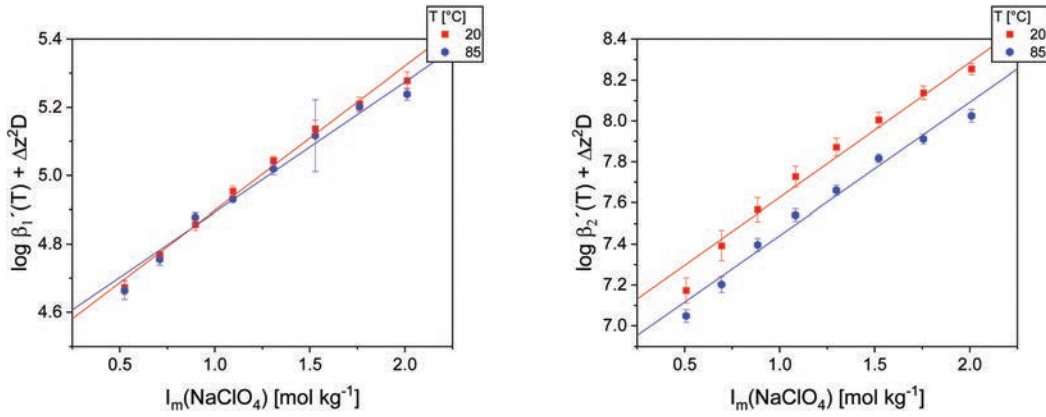


Fig. 6 Ionic strength dependence of $\log \beta'_n(T) - \Delta z^2 D$ and linear fitting of the data according to the SIT for the complexation reactions $\text{NpO}_2^+ + n\text{Ox}^{2-} \rightleftharpoons \text{NpO}_2(\text{Ox})_n^{1-2n}$ ($n = 1, 2$) in NaClO_4 . $T = 20, 85$ °C.

to eqn (6) yielding the thermodynamic stability constants $\log \beta_n^0(T)$.⁶⁸

$$\log \beta'_n(T) - \Delta z^2 D = \log \beta_n^0(T) + \Delta \varepsilon I_m \quad (6)$$

D is the Deby-Hückel term, Δz^2 is the sum of the charges z of the chemical species and $\Delta \varepsilon$ is the sum of the binary ion-ion interaction coefficients $\varepsilon(j,k)$ of the educts and products. A linear correlation of $\log \beta'_n(T) - \Delta z^2 D$ with I_m is observed for all studied temperatures in both studied electrolytes (NaCl and NaClO_4). In Fig. 6 the SIT plots for $T = 20$ and 85 °C and NaClO_4 media are displayed as examples.

The calculated $\log \beta_n^0(T)$ are listed in Table 2. For both electrolytes the obtained $\log \beta_n^0(T)$ values are in excellent agreement and averaged (“Ø”) $\log \beta_n^0(T)$ values are calculated. In case of the first stability constant $\log \beta_1^0(T)$ only a weak temperature dependence is observed. In contrast, $\log \beta_2^0(T)$ decreases significantly with increasing temperature. Thus, the formation of $\text{NpO}_2(\text{Ox})_2^{3-}$ is clearly exothermic.

In Fig. 7 the temperature dependence of the averaged $\log \beta_n^0(T)$ is displayed as a function of the reciprocal temperature T^{-1} . The data correlate linearly with T^{-1} indicating that the reaction enthalpies $\Delta_r H_{n,m}^0$ for both complexation steps are constant in the studied temperature interval. Thus, the temperature dependence can be described by the integrated van't Hoff equation (eqn (7)).

$$\log \beta_n^0(T) = \log \beta_n^0(T_0) + \frac{\Delta_r H_{n,m}^0(T_0)}{R \ln(10)} \left(\frac{1}{T_0} - \frac{1}{T} \right) \quad (7)$$

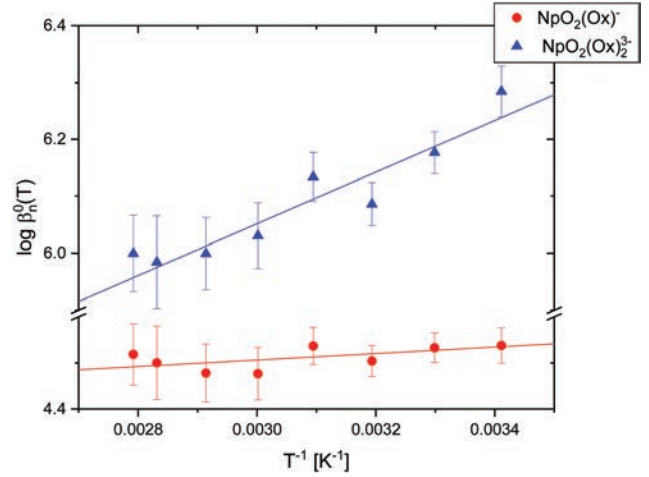


Fig. 7 Plot of $\log \beta_n^0(T)$ ($n = 1, 2$) as a function of the reciprocal temperature and fitting according to the integrated van't Hoff equation.

With R being the universal gas constant and $T_0 = 298.15$ K. Linear regression analyses according to eqn (7) yield the standard reaction enthalpy $\Delta_r H_{n,m}^0$ of the complexation reactions. The standard reaction entropy $\Delta_r S_{n,m}^0$ is calculated using eqn (8).

$$\Delta_r G_{n,m}^0 = \Delta_r H_{n,m}^0 - T \times \Delta_r S_{n,m}^0 = RT \ln \beta_n^0 \quad (8)$$

This approach is valid for small temperature intervals ($\Delta T = 100$ K) assuming $\Delta_r C_{m,p}^0 = 0$ and $\Delta_r H_{n,m}^0 = \text{const}$. The deter-

Table 2 Thermodynamic stability constants $\log \beta_n^0(T)$ for the formation of $[\text{NpO}_2(\text{Ox})_n]^{1-2n}$ ($n = 1, 2$) obtained from NaClO_4 and NaCl media and mean values (“Ø”) as a function of temperature

	T [°C]	20	30	40	50	60	70	80	85
$\text{NpO}_2(\text{Ox})^-$	NaClO_4	4.48 ± 0.07	4.49 ± 0.08	4.48 ± 0.07	4.48 ± 0.06	4.48 ± 0.10	4.46 ± 0.09	4.48 ± 0.10	4.49 ± 0.09
	NaCl	4.59 ± 0.05	4.58 ± 0.04	4.53 ± 0.04	4.59 ± 0.05	4.47 ± 0.07	4.50 ± 0.08	4.53 ± 0.11	4.55 ± 0.09
	Ø	4.54 ± 0.08	4.53 ± 0.09	4.50 ± 0.09	4.54 ± 0.08	4.48 ± 0.12	4.48 ± 0.12	4.50 ± 0.15	4.52 ± 0.13
$\text{NpO}_2(\text{Ox})_2^{3-}$	NaClO_4	6.26 ± 0.05	6.23 ± 0.06	6.18 ± 0.05	6.15 ± 0.05	6.11 ± 0.07	6.06 ± 0.07	6.03 ± 0.07	6.05 ± 0.07
	NaCl	6.31 ± 0.04	6.12 ± 0.03	5.99 ± 0.03	6.11 ± 0.04	5.95 ± 0.05	5.94 ± 0.06	5.94 ± 0.08	5.94 ± 0.06
	Ø	6.28 ± 0.07	6.18 ± 0.07	6.09 ± 0.06	6.13 ± 0.06	6.03 ± 0.09	6.00 ± 0.09	5.98 ± 0.11	6.00 ± 0.09

Table 3 Thermodynamic functions for the formation of $\text{NpO}_2(\text{Ox})_n^{1-2n}$ ($n = 1, 2$) according to eqn (7)

Electrolyte	$\text{NpO}_2(\text{Ox})_n^{1-2n}$	$\log \beta_n^0(25\text{ }^\circ\text{C})$	$\Delta_r H_{n,m}^0$ [kJ mol^{-1}]	$\Delta_r S_{n,m}^0$ [$\text{J mol}^{-1}\text{K}^{-1}$]	$\Delta \epsilon$
NaClO_4	$n = 1$	4.49 ± 0.08	0.6 ± 0.6	84 ± 4	0.39 ± 0.04
	$n = 2$	6.24 ± 0.11	7.3 ± 0.7	95 ± 9	0.52 ± 0.04
NaCl	$n = 1$	4.58 ± 0.14	1.9 ± 0.4	79 ± 16	0.18 ± 0.03
	$n = 2$	6.20 ± 0.09	10.0 ± 1.8	85 ± 11	0.20 ± 0.06
\emptyset	$n = 1$	4.53 ± 0.12	1.3 ± 0.7	82 ± 2	
	$n = 2$	6.22 ± 0.24	8.7 ± 1.4	90 ± 5	

mined $\Delta_r H_{n,m}^0$ and $\Delta_r S_{n,m}^0$ values are summarized in Table 3. The obtained data reveal that both complexation steps are exothermic and entropy driven.

In the literature no temperature dependent $\log \beta_n^0(T)$ values are reported. The available data were determined by different experimental techniques like spectrophotometry or solvent extraction and are mostly limited to 25 °C.^{31–33,68,72} In Table 4 literature values are compared to the results of the present work. In case of $\text{NpO}_2(\text{Ox})^-$ the $\log \beta_1^0(25\text{ }^\circ\text{C})$ values in the literature vary between 3.84 and 4.40 and are lower than the present result. The $\log \beta_2^0(T)$ values of $\text{NpO}_2(\text{Ox})_2^{3-}$ range between 5.8 and 7.36 in the literature. The value of the present work fits perfectly within this interval. Definite reasons for the wide scattering of the stability constants in the literature cannot be figured out. One possibility might be the application of different experimental techniques. Comparing the data reported by Patil *et al.* determined by spectrophotometry and cation exchange a discrepancy for $\log \beta_1^0$ of 0.47 and for $\log \beta_2^0$ of 0.30 is observed within this single survey.³¹ Comparison of the spectroscopically determined $\log \beta_1^0$ values reported by Patil *et al.* with the data of Tian *et al.* shows a good accordance of these data.^{31,32} Nevertheless, they are lower by approximately 0.6 logarithmic units compared to the present result. The $\log \beta_2^0$ values of Patil *et al.* and Tian *et al.* differ significantly by 1.06. Compared to the present results the reported $\log \beta_2^0$ value by Tian *et al.* is in excellent accordance. However, the $\log \beta_n^0$ values determined by Tian *et al.* are obtained from single point extrapolation of conditional data derived at

Table 4 Thermodynamic stability constants the formation of $\text{NpO}_2(\text{Ox})_n^{1-2n}$ ($n = 1, 2$) and comparison with literature data

Complex	Method/data base	$\log \beta_n^0(25\text{ }^\circ\text{C})$	Ref.
$\text{NpO}_2(\text{Ox})^-$	sp	4.53 ± 0.12	p.w.
	cix	4.40	31
	sp	3.93	31
	sp	4.08 ± 0.11	32
	sx	3.84	33
	NEA TDB	3.9 ± 0.1	68
	NIST	3.9	72
$\text{NpO}_2(\text{Ox})_2^{3-}$	sp	6.22 ± 0.24	p.w.
	cix	7.36	31
	sp	7.06	31
	sp	6.12 ± 0.21	32
	NEA TDB	5.8 ± 0.2	68
	NIST	5.8	72

Methods: sp: spectrophotometry; sx: solvent extraction; cix: cation exchange.

$I_m = 1.05\text{ mol kg}^{-1}\text{ NaClO}_4$.³² In our work conditional $\log \beta'_n$ at various I_m were determined and extrapolated by the SIT to $I_m = 0$. For extrapolation Tian *et al.* used the reported $\epsilon_{j,k}$ values given in the NEA-TDB (A detailed discussion of the $\epsilon_{j,k}$ values in the NEA-TDB is given in the section 3.1.5).^{18,32} The deviation of the present results from the values given in the NEA-TDB and the NIST most likely originates from the wide scattering of the $\log \beta'(I_m)$ values used in the data bases for the SIT extrapolation and the resulting poor linearity of the $\log \beta' - \Delta z^2$ vs. I_m plots to calculate $\log \beta^0$.

Thermodynamic $\Delta_r H_{n,m}^0$ and $\Delta_r S_{n,m}^0$ values are not available in the literature. Only one study by Tian *et al.* provides conditional $\Delta_r H'_{n,m}$ and $\Delta_r S'_{n,m}$ values determined by spectrophotometry and micro calorimetry at $I_m(\text{NaClO}_4) = 1.05$.³² A comparison of these values with the results of the present work at equal experimental conditions is given in Table 5. First of all, the $\log \beta'_n(25\text{ }^\circ\text{C})$ values of the present work are by approximately 0.5–0.6 logarithmic units higher compared to the literature. Nevertheless, the reported $\Delta_r H'_{1,m}$ is in very good agreement with the present value whereas the $\Delta_r H'_{2,m}$ values show significant deviations. The literature reports more exothermic formation of $\text{NpO}_2(\text{Ox})_2^{3-}$. Comparison of the $\Delta_r S'_{n,m}$ values reveals that the results of the present work are higher compared to the literature. This deviation might originate from the discrepancies in the $\log \beta'_n(25\text{ }^\circ\text{C})$ values.

3.1.5 Ionic strength dependence. In addition to the thermodynamic functions ($\log \beta_n^0(T)$, $\Delta_r H_{n,m}^0$, $\Delta_r S_{n,m}^0$) at IUPAC reference state conditions, application of the SIT yields the stoichiometric sum of the binary ion–ion interaction coefficients of the complexation reactions ($\Delta \epsilon_1^0(T)$ and $\Delta \epsilon_2^0(T)$) as a function of the temperature. The $\Delta \epsilon_1^0(T)$ and $\Delta \epsilon_2^0(T)$ values for the formation of $\text{NpO}_2(\text{Ox})_n^{1-2n}$ ($n = 1, 2$) in NaClO_4 and NaCl

Table 5 Conditional stability constants $\log \beta'(25\text{ }^\circ\text{C})$ and thermodynamic functions $\Delta_r H'_{n,m}$ and $\Delta_r S'_{n,m}$ and comparison with literature data at $I_m = 1.0\text{ mol kg}^{-1}$

Complex	Method	$\log \beta'_n(25\text{ }^\circ\text{C})$	$\Delta_r H'_{n,m}$ [kJ mol^{-1}]	$\Delta_r S'_{n,m}$ [$\text{J mol}^{-1}\text{K}^{-1}$]	Ref.
$\text{NpO}_2(\text{Ox})^-$	sp	4.12 ± 0.10	9.7 ± 3.4	48 ± 3	p.w.
	sp	3.57 ± 0.02	7.0 ± 0.9		32
	cal		12.2 ± 0.1	27.4 ± 0.6	32
$\text{NpO}_2(\text{Ox})_2^{3-}$	sp	6.81 ± 0.31	14.1 ± 2.6	84 ± 8	p.w.
	sp	6.23 ± 0.02	19.6 ± 1.7		32
	cal		25.5 ± 0.1	33.7 ± 0.9	32

Methods: sp: spectrophotometry; cal: micro calorimetry.

media are displayed in Fig. 8. Within the error, the scattering of the $\Delta\epsilon_n^0(T)$ values observed for both electrolytes agrees with various studies on the ionic strength dependence of the complexation of Np(v) or trivalent lanthanides and actinides and only a marginal temperature dependence between 20–85 °C is observed.^{36,69,71,73,74} Thus, averaged temperature-independent $\Delta\epsilon_{j,k}$ values are calculated for both background electrolytes (NaCl, NaClO₄). The averaged values are given in Table 3. According to the SIT the temperature independent binary ion–ion interaction coefficients $\epsilon_{j,k}$ of the different Np(v)–oxalate complexes with Na⁺ are calculated (eqn (9)).

$$\Delta\epsilon = \sum \epsilon_{\text{products}} - \sum \epsilon_{\text{educt}} \quad (9)$$

The binary ion–ion interaction coefficients $\epsilon(\text{Na}^+, \text{Ox}^{2-}) = 0.03 \pm 0.01$, $\epsilon(\text{NpO}_2^+, \text{ClO}_4^-) = 0.25 \pm 0.05$, and $\epsilon(\text{NpO}_2^+, \text{Cl}^-) = 0.09 \pm 0.05$ reported in the NEA-TDB are used for this purpose.²⁷ The calculated values are listed below:

$$\epsilon_{\text{NaCl}}(\text{Na}^+, \text{NpO}_2(\text{Ox})^-) = 0.17 \pm 0.06,$$

$$\epsilon_{\text{NaClO}_4}(\text{Na}^+, \text{NpO}_2(\text{Ox})^-) = 0.22 \pm 0.06,$$

$$\epsilon_{\text{NaCl}}(\text{Na}^+, \text{NpO}_2(\text{Ox})_2^{3-}) = 0.27 \pm 0.08,$$

$$\epsilon_{\text{NaClO}_4}(\text{Na}^+, \text{NpO}_2(\text{Ox})_2^{3-}) = 0.43 \pm 0.09$$

Comparison of the $\epsilon_{j,k}$ values for the two complex species shows slight deviations between the values obtained in NaCl and NaClO₄ media. In case of the 1 : 1 complex the deviation is 0.05 which is within the error range of the $\epsilon_{j,k}$ values. In case of the 1 : 2 complex a deviation of 0.16 is observed. This discrepancy can be explained by a defective $\epsilon(\text{NpO}_2^+, \text{ClO}_4^-) = 0.25 \pm 0.05$ reported in the NEA-TDB.²⁷ This assumption is based on similar observations for the complexation of Np(v) with formate, acetate, chloride and fluoride.^{55,70,71,75} Nonetheless, the obtained $\log \beta_n^0(T)$ values and thermodynamic functions for the formation of the Np(v)–oxalate complexes determined in NaCl and NaClO₄ media are in excellent agreement. This confirms that the ionic strength dependency of the complex

formation is accurately described in both background electrolytes using the determined $\Delta\epsilon_{j,k}$ values.

Within the NEA-TDB review conditional stability constants at various ionic strengths and 20–25 °C from different studies were compared and extrapolated to $I_m = 0$ yielding an $\epsilon(\text{Na}^+, \text{NpO}_2(\text{Ox})^-) = -0.4 \pm 0.1$ and $\epsilon(\text{Na}^+, \text{NpO}_2(\text{Ox})_2^{3-}) = -0.3 \pm 0.2$.¹⁸ These $\epsilon_{j,k}$ values deviate significantly from the values determined in the present work. This discrepancy most likely originates from the wide scattering of the $\log \beta'$ values used in the NEA-TDB for the SIT extrapolation and the resulting poor linearity of the $\log \beta' - \Delta z^2$ vs. I_m plots. In contrast, the $\epsilon_{j,k}$ values determined in the present work are based on a consistent data set resulting in fits with superior quality and more reliable data.

3.2 Structural investigation

Oxalate is the simplest dicarboxylate available and can either coordinate only *via* one COO⁻ group (end-on mode) or *via* both COO⁻ groups toward the metal ion forming chelate complexes (side-on mode) In Fig. 9 the structures of the complexes with the two coordination modes are sketched. The equatorial coordination number accounts for 5. Free coordination places in the equatorial plane are occupied by water molecules. These are omitted for clarity in Fig. 9. Valuable structural data of the complexes and information on the coordination mode of oxalate can be obtained by EXAFS analysis.

3.2.1 EXAFS data analysis. In Fig. 10 the k^2 -weighted Np-L₃-edge EXAFS spectra of the Np(v)–oxalate complexes, their



Fig. 9 Schematic structures of the optimized Np(v) oxalate complexes ($n = 1, 2$). Water molecules are omitted for clarity.

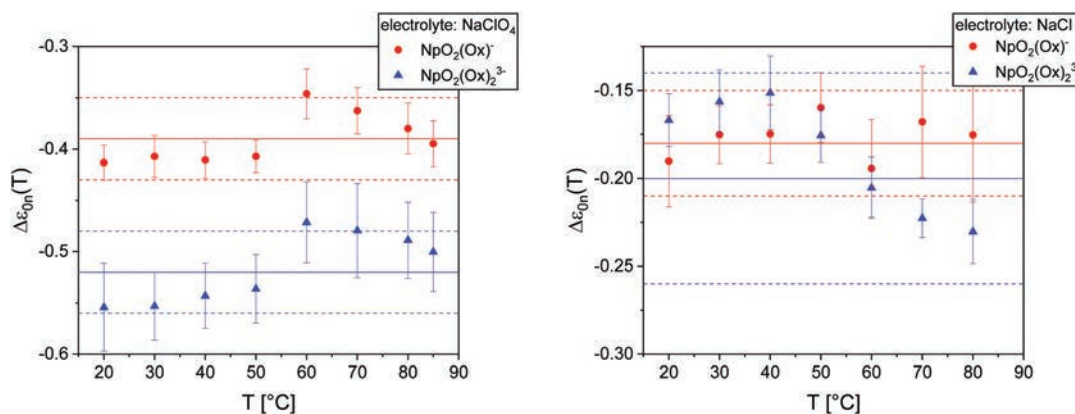


Fig. 8 $\Delta\epsilon_n^0(T)$ values for the formation of $[\text{NpO}_2(\text{Ox})_n]^{1-2n}$ ($n = 1, 2$) in NaClO₄ (left) and NaCl (right) as a function of the temperature. The error range (dashed lines) equal the 1σ error of the mean value.

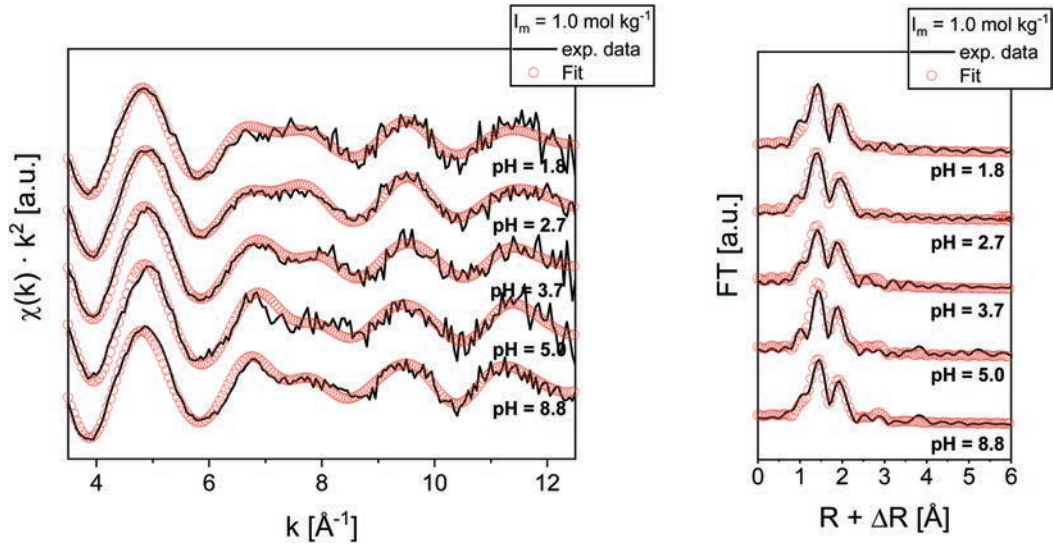


Fig. 10 Raw k^2 weighted Np L_3 edge EXAFS spectra (left) and Fourier transforms (right) of Np(V) in the presence of oxalate as a function of pH_c (black) together with the best fit from EXAFSPAK (red circles).

Fourier transformations and the corresponding fit curves are displayed as a function of the pH_c value. The results of the fits and the fit parameters are listed in Table 6. The spectra are dominated by the axial and equatorial O-atoms (O_{ax} , O_{eq}) which are located at $1.83 \pm 0.02 \text{ \AA}$ (O_{ax}) and $2.45 \pm 0.02 \text{ \AA}$ (O_{eq}). These results are in excellent agreement with literature data.^{36,76,77} The coordination number of the Np(V) ion is in good accordance with the expected value of 5 within the studied pH range.^{77,78} With increasing pH_c the coordination number and the O_{ax} and O_{eq} distances remain constant. The coordination mode of the oxalate molecules toward the Np(V) centre is determined using the distances of the carboxylic carbon atoms (C_c). An averaged value of $3.32 \pm 0.06 \text{ \AA}$ is obtained within the studied pH range. Their coordination number increases with increasing pH_c which is in excellent agreement with the results of the speciation studies by Vis/NIR. EXAFS studies by Takao *et al.* and Vasiliev *et al.* on the complexation of Np(V) with acetate and propionate show C_c distances of $2.91 \pm 0.02 \text{ \AA}$ and $2.87 \pm 0.03 \text{ \AA}$.^{36,76} As acetate and

propionate are monocarboxylates these distances correspond to a bidentate coordinating COO^- group (end-on coordination). The C_c distances determined herein for the $\text{NpO}_2(\text{Ox})_n^{1-2n}$ complexes are about $0.4\text{--}0.5 \text{ \AA}$ longer compared to the C_c distances of the acetate and propionate complexes indicating a different coordination mode of oxalate. Recently, we investigated the complexation of Np(V) with formate by EXAFS.⁷⁵ In this study an averaged C_c distance of $3.39 \pm 0.07 \text{ \AA}$ was determined. This distance was attributed to a monodentate coordination of formate with only one O-atom of the carboxylic group. This distance is in good agreement with the results for the oxalate complexes in the present work. Thus, the oxalate molecules coordinate *via* one O-atom of each COO^- group toward the Np(V) centre forming five membered chelate rings. The coordination mode is not affected by the pH.

3.2.2 Quantum chemical calculations. The interpretation of the EXAFS results is verified by quantum chemical calculations. The determined bond distances of the optimized molecular structures of the five-fold coordinated $\text{NpO}_2(\text{Ox})^-$

Table 6 Fit parameters of the k^2 weighted Np L_3 edge EXAFS spectra shown in Fig. 8

pH		1.8	2.7	3.7	5.0	8.8
O_{ax}	N	2^a	2^a	2^a	2^a	2^a
	$R/\text{\AA}$	1.83 ± 0.01	1.82 ± 0.1	1.82 ± 0.01	1.84 ± 0.01	1.85 ± 0.01
	$\sigma^2/\text{\AA}^2$	0.0019 ± 0.0001	0.0007 ± 0.0002	0.0017 ± 0.0004	0.0002 ± 0.0004	0.0008 ± 0.0002
O_{eq}	N	4.5 ± 1.0	3.6 ± 1.0	4.5 ± 1.0	5.3 ± 1.0	4.1 ± 1.0
	$R/\text{\AA}$	2.47 ± 0.01	2.48 ± 0.01	2.44 ± 0.01	2.43 ± 0.01	2.45 ± 0.01
	$\sigma^2/\text{\AA}^2$	0.0062 ± 0.0015	0.0044 ± 0.0019	0.0061 ± 0.0013	0.0085 ± 0.0020	0.0045 ± 0.0008
C_c	N	0.9 ± 1.0	1.5 ± 1.0	2.2 ± 1.0	3.3 ± 1.0	3.3 ± 1.0
	$R/\text{\AA}$	3.47 ± 0.03	3.47 ± 0.03	3.30 ± 0.03	3.32 ± 0.03	3.39 ± 0.02
	$\sigma^2/\text{\AA}^2$	0.004^a	0.004^a	0.004^a	0.004^a	0.004^a
$\Delta E_0/\text{eV}$		10.5 ± 0.7	12.9 ± 0.3	10.7 ± 0.5	10.8 ± 0.7	10.7 ± 0.4
Red error		0.0207544	0.00722427	0.0167346	0.0261492	0.0101572

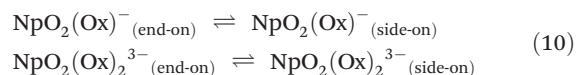
^a Parameter fixed; O_{ax} axial O atoms, O_{eq} equatorial O atoms, C_c C atoms of coordinating COO^- groups.

Table 7 Distances of the ligands atoms toward the metal centre. Results of the quantum chemical calculations compared to EXAFS data

Method	Complex	Coord. mod.	O _{ax} [Å]	O _{eq} [Å]	C _c [Å]
DFT	NpO ₂ (Ox) ⁻	End on	1.84	2.47	2.84
		Side on	1.83	2.46	3.26
	NpO ₂ (Ox) ₂ ³⁻	End on	1.82	2.47	2.86
		Side on	1.83	2.44	3.29
EXAFS	NpO ₂ (Ox) ⁻ /NpO ₂ (Ox) ₂ ³⁻		1.83 ± 0.02	2.45 ± 0.02	3.39 ± 0.07

and NpO₂(Ox)₂³⁻ complexes with end-on and side-on coordinating oxalate molecules (see Fig. 9) are summarized in Table 7 and compared to the EXAFS results. The experimentally obtained distances for O_{ax} and O_{eq} are in excellent accordance with the results of the structure optimizations. The distances are 1.83 ± 0.01 Å (O_{ax}) and 2.46 ± 0.01 Å (O_{eq}). The calculated C_c distances for end-on and side-on coordination of oxalate are 2.85 ± 0.01 Å and 3.28 ± 0.02 Å, respectively. Thus, the structure optimizations confirm the interpretation of the EXAFS data that oxalate coordinates in a side-on mode forming five membered chelate rings in the equatorial plane with Np(v).

Additionally, calculations on isomerisation reactions for an end-on into a side-on coordinated oxalate according to eqn (10) are performed.



The theoretical approximation of the Gibbs free energies ΔG for the isomerisation reactions according to eqn (10) are listed in Table 8. The ΔG values are calculated using the difference of the ground state energies ΔE_g on MP2 level with thermodynamic corrections ΔE_{vib} and solvation effects ΔE_{solv} taken into account: $\Delta G = \Delta E_g + \Delta E_{\text{vib}} + \Delta E_{\text{solv}}$ ($\Delta E = E_{\text{end-on}} - E_{\text{side-on}}$) (see eqn (11)):

$$\begin{aligned} DG &= G_{\text{end-on}} - G_{\text{side-on}} \\ &= E_{g(\text{end-on})} - E_{g(\text{side-on})} + E_{\text{vib}(\text{end-on})} \\ &\quad - E_{\text{vib}(\text{side-on})} + E_{\text{solv}(\text{end-on})} - E_{\text{solv}(\text{side-on})} \\ &= \Delta E_g + \Delta E_{\text{vib}} + \Delta E_{\text{solv}} \end{aligned} \quad (11)$$

The results show negative ΔG values (NpO₂(Ox)⁻: -32.93 kJ mol⁻¹; NpO₂(Ox)₂³⁻: -84.34 kJ mol⁻¹) for both isomerisation reactions. Thus, the formation of chelate complexes with the oxalate coordinating in a side-on mode toward the Np(v) ion is energetically preferred compared to an end-on coordination *via* only one COO⁻ group of the ligand. This is again in excellent agreement with the EXAFS results.

The determined coordination mode of oxalate by EXAFS and the quantum chemical calculations provides an excellent explanation for the observed thermodynamic behaviour of the complexation reactions. The formation of chelate complexes is usually directed by significantly lower $\Delta_r H_{n,m}^0$ values.⁷⁹

4 Summary and conclusion

In the present work stability constants and thermodynamic functions for the complex formation of Np(v) with oxalate are determined. The complexation is studied systematically as a function of the ligand concentration ([Ox²⁻]_{total}), ionic strength (NaCl and NaClO₄) and temperature (20–85 °C) by absorption spectroscopy in the near infrared region. The formation of exclusively two different Np(v) oxalate complexes with a stoichiometry of NpO₂(Ox)_n¹⁻²ⁿ ($n = 1, 2$) is observed at the studied experimental conditions. The stoichiometry of the formed complexes is confirmed by slope analyses according to the law of mass action. With increasing temperature the equilibrium of the complexation reaction shifts toward the Np(v) aquo ion and the formation of NpO₂(Ox)_n¹⁻²ⁿ is repressed at elevated temperatures. This is reflected by a decrease of the stability constants. The $\log \beta_1^0(25 \text{ °C}) = 4.53 \pm 0.12$ decreases by about 0.1 and $\log \beta_2^0(25 \text{ °C}) = 6.22 \pm 0.24$ decreases by about 0.3. The thermodynamic stability constants correlate linearly with T^{-1} and the reactions enthalpies and entropies are calculated with the integrated van't Hoff equation. The results show that the complexation reactions are exothermic with $\Delta_r H_{1,m}^0 = -9.7 \pm 3.4 \text{ kJ mol}^{-1}$ and $\Delta_r H_{2,m}^0 = -14.1 \pm 2.6 \text{ kJ mol}^{-1}$. Furthermore, the $\Delta \epsilon_1^0$ and $\Delta \epsilon_2^0$ values are determined as a function of temperature for two different ionic media (NaCl and NaClO₄) using the SIT. No significant temperature dependence of $\Delta \epsilon_1^0$ and $\Delta \epsilon_2^0$ is observed and the respective binary ion-ion interaction coefficients $\epsilon_{j,k}$ are calculated.

Structural investigations by EXAFS spectroscopy and quantum chemical calculations provide information on the coordination mode of oxalate toward the Np(v) ion. The experiments and calculations confirm a side-on coordination of

Table 8 Gibbs free energies for the isomerisation reactions according to eqn (10) and (11). Ground state energies E_g calculated on MP2 level

Complex	ΔE_g [kJ mol ⁻¹]	ΔE_{vib} [kJ mol ⁻¹]	ΔE_{solv} [kJ mol ⁻¹]	ΔG [kJ mol ⁻¹]
NpO ₂ (Ox) ⁻	34.35	6.13	4.71	32.93
NpO ₂ (Ox) ₂ ³⁻	170.71	44.74	41.64	84.34

oxalate toward the Np(v) ion and the formation of five membered chelate rings.

The present work is a detailed spectroscopic and quantum chemical study focusing on thermodynamic functions for the complexation reactions of Np(v) with oxalate and the structures of the formed complex species. The studied ligand system serves as model for macromolecular organic compounds and the derived data improve the knowledge of the complexation properties of An(v) with polyfunctional macromolecular organic compounds on a molecular level. Furthermore, the present results are a valuable contribution to the thermodynamic database of actinides improving the scientific basis for describing the aquatic chemistry of actinide ions at conditions relevant for nuclear waste disposal.

Conflicts of interest

There are no conflicts to declare.

Acknowledgements

All spectroscopic measurements were carried out at the Institute for Nuclear Waste Disposal (INE) at Karlsruhe Institute of Technology (KIT). Dr D. Fellhauer and Dr M Altmaier are acknowledged for providing the ²³⁷Np and their experimental support. The KIT Institute for Beam Physics and Technology (IBPT) is acknowledged for the operation of the storage ring, the Karlsruhe Research Accelerator (KARA), and provision of beamtime at the KIT light source. This work is supported by the German Federal Ministry for Economic Affairs and Energy (BMWi) under contract 02E11415H and the German Federal Ministry of Education and Research (BMBF) under contract 02NUK039C.

References

- 1 H. Geckeis, K.-J. Röhligh and K. Mengel, Endlagerung radioaktiver Abfälle, *Chem. Unserer Zeit*, 2012, **46**(5), 282–293.
- 2 W. Runde, The chemical interactions of actinides in the environment, *Los Alamos Sci.*, 2000, **26**, 392–411.
- 3 OECD and N. E. Agency, *Considering Timescales in the Post-closure Safety of Geological Disposal of Radioactive Waste*, 2009.
- 4 H. Geckeis, J. Lutzenkirchen, R. Polly, T. Rabung and M. Schmidt, Mineral-water interface reactions of actinides, *Chem. Rev.*, 2013, **113**(2), 1016–1062.
- 5 R. Gens, P. Lalieux, P. D. Preter, A. Dierckx, J. Bel, J.-P. Boyazis and W. Cool, The Second Safety Assessment and Feasibility Interim Report (SAFIR 2 Report) on HLW Disposal in Boom Clay: Overview of the Belgian Programme, *MRS Proc.*, 2011, **807**, 917–924.
- 6 N. E. A. Oecd, *Safety of Geological Disposal of High-level and Long-lived Radioactive Waste in France*, Nuclear Energy Agency Organisation for Economic Co-operation and Development, 2006.
- 7 P. Hoth, H. Wirth, K. Reinhold, V. Bräuer, P. Krull and H. Feldrappe, *Endlagerung radioaktiver Abfälle in tiefen geologischen Formationen Deutschlands – Untersuchung und Bewertung von Tongesteinsformationen*, BGR Bundesanstalt für Geowissenschaften und Rohstoffe, Hannover/Germany, 2007.
- 8 P. Birkhäuser, et al., *NAGRA Projekt Opalinuston – Synthese der geowissenschaftlichen Untersuchungsergebnisse, Entsorgungsnachweis für abgebrannte Brennelemente, verglaste hochaktive sowie langlebige mittelaktive Abfälle*, NAGRA Nationale Genossenschaft für die Lagerung radioaktiver Abfälle, Wettingen/Switzerland, 2002.
- 9 K. Mengel, K.-J. Röhligh and H. Geckeis, Endlagerung radioaktiver Abfälle, *Chem. Unserer Zeit*, 2012, **46**(4), 208–217.
- 10 K.-J. Röhligh, H. Geckeis and K. Mengel, Endlagerung radioaktiver Abfälle, *Chem. Unserer Zeit*, 2012, **46**(3), 140–149.
- 11 F. D. Hansen and C. D. Leigh, *Salt disposal of heat-generating nuclear waste*, Sandia National Laboratories Albuquerque, NM, 2011.
- 12 E. Gaucher, C. Robelin, J. M. Matray, G. Negral, Y. Gros, J. F. Heitz, A. Vinsot, H. Rebours, A. Cassagnabere and A. Bouchet, ANDRA underground research laboratory: interpretation of the mineralogical and geochemical data acquired in the Callovian-Oxfordian formation by investigative drilling, *Phys. Chem. Earth*, 2004, **29**(1), 55–77.
- 13 T. R. Allen, R. E. Stoller and S. Yamanaka, *Comprehensive Nuclear Materials*, Elsevier, Radarweg 29, PO Box 211, 1000 AE Amsterdam, The Netherlands, 2012.
- 14 A. Courdouan, I. Christl, S. Meylan, P. Wersin and R. Kretzschmar, Isolation and characterization of dissolved organic matter from the Callovo-Oxfordian formation, *Appl. Geochem.*, 2007, **22**(7), 1537–1548.
- 15 A. Courdouan, I. Christl, S. Meylan, P. Wersin and R. Kretzschmar, Characterization of dissolved organic matter in anoxic rock extracts and in situ pore water of the Opalinus Clay, *Appl. Geochem.*, 2007, **22**(12), 2926–2939.
- 16 E. M. Thurman, *Organic Geochemistry of Natural Waters*, Springer, Dordrecht, 1985.
- 17 S. A. Wood, The aqueous geochemistry of the rare-earth elements: Critical stability constants for complexes with simple carboxylic acids at 25 °C and 1 bar and their application to nuclear waste management, *Eng. Geol.*, 1993, **34**(3–4), 229–259.
- 18 W. Hummel, G. Anderegg, L. Rao, I. Puigdomenech and O. Tochiyama, *Chemical Thermodynamics of Compounds and Complexes of U, Np, Pu, Am, Tc, Se, Ni and Zr with Selected Organic Ligands*, Elsevier B.V., 2005.
- 19 M. Schnitzer and S. U. Khan, *Humic substances in the environment*, M. Dekker, 1972.
- 20 G. R. Choppin, The role of natural organics in radionuclide migration in natural aquifer systems, *Radiochim. Acta*, 1992, **58**(1), 113–120.
- 21 M. Hakanen and H. Ervanne, *The influence of organic cement additives on radionuclide mobility A literature survey*, Finland, 2006, pp. 42.

- 22 B. F. Greenfield, D. J. Ilett, M. Ito, R. McCrohon, T. G. Heath, C. J. Tweed, S. J. Williams and M. Yui, The Effect of Cement Additives on Radionuclide Solubilities, *Radiochim. Acta*, 1998, **82**(s1), 27–32.
- 23 I. A. E. AGENCY, *Geological Disposal of Radioactive Waste*, International Atomic Energy Agency, Vienna, 2006.
- 24 D. Bosbach, B. Luckscheiter, B. Brendebach, M. A. Denecke and N. Finck, High level nuclear waste glass corrosion in synthetic clay pore solution and retention of actinides in secondary phases, *J. Nucl. Mater.*, 2009, **385**(2), 456–460.
- 25 W. Brewitz, *Ablauf und Ergebnisse der Eignungsuntersuchung der Schachanlage Konrad für die Endlagerung radioaktiver Abfälle: Zusammenfassung*, Gesellschaft für Strahlen-und Umweltforschung, 1982.
- 26 M. H. Bradbury and B. Baeyens, *Derivation of in situ opalinus clay porewater compositions from experimental and geochemical modelling studies*, 1019–0643, Switzerland, 1997, p. 60.
- 27 R. Guillaumont, T. Fanghänel, V. Neck, J. Fuger and D. A. Palmer, *Update on the Chemical Thermodynamics of Uranium, Neptunium, Plutonium, Americium and Technetium*, Elsevier B.V., 2003.
- 28 R. J. Lemire, *Chemical thermodynamics of neptunium and plutonium*, Elsevier, 2001, vol. 4.
- 29 G. R. Choppin, Actinide speciation in the environment, *J. Radioanal. Nucl. Chem.*, 2007, **273**(3), 695–703.
- 30 K. Maher, J. R. Bargar and G. E. Brown Jr., Environmental speciation of actinides, *Inorg. Chem.*, 2013, **52**(7), 3510–3532.
- 31 S. K. Patil, V. V. Ramakrishna and M. V. Ramaniah, Aqueous coordination complexes of neptunium, *Coord. Chem. Rev.*, 1978, **25**(2), 133–171.
- 32 G. Tian and L. Rao, Complexation of Np(v) with oxalate at 283–343 K: spectroscopic and microcalorimetric studies, *Dalton Trans.*, 2012, **41**(2), 448–452.
- 33 O. S. Pokrovsky and G. R. Choppin, Neptunium(v) Complexation by Acetate, Oxalate and Citrate in NaClO₄ Media at 25 °C, *Radiochim. Acta*, 1997, **79**(3), 167–171.
- 34 A. E. Martell, R. M. Smith and R. J. Motekaitis, *NIST standard reference database 46 version 8.0: NIST critically selected stability constants of metal complexes*, U.S. Department of Commerce, Technology Administration, National Institute of Standards and Technology, Standard Reference Data Program, Gaithersburg, MD, 2004.
- 35 D. Fellhauer, J. Rothe, M. Altmaier, V. Neck, J. Runke, T. Wiss and T. Fanghänel, Np(v) solubility, speciation and solid phase formation in alkaline CaCl₂ solutions. Part I: Experimental results, *Radiochim. Acta*, 2016, **104**(6), 355–379.
- 36 A. N. Vasiliev, N. L. Banik, R. Marsac, D. R. Fröhlich, J. Rothe, S. N. Kalmykov and C. M. Marquardt, Np(v) complexation with propionate in 0.5–4 M NaCl solutions at 20–85 degrees C, *Dalton Trans.*, 2015, **44**(8), 3837–3844.
- 37 M. Altmaier, V. Metz, V. Neck, R. Müller and T. Fanghänel, Solid-liquid equilibria of Mg(OH)₂(cr) and Mg₂(OH)₃Cl·4H₂O(cr) in the system Mg-Na-H-OH-Cl-H₂O at 25 °C, *Geochim. Cosmochim. Acta*, 2003, **67**(19), 3595–3601.
- 38 M. A. Denecke, J. Rothe, K. Dardenne, H. Blank and J. Hormes, The INE Beamline for Actinide Research at ANKA, *Phys. Scr.*, 2005, 1001–1003.
- 39 J. Rothe, S. Butorin, K. Dardenne, M. A. Denecke, B. Kienzler, M. Loble, V. Metz, A. Seibert, M. Steppert, T. Vitova, C. Walther and H. Geckeis, The INE-Beamline for actinide science at ANKA, *Rev. Sci. Instrum.*, 2012, **83**(4), 043105.
- 40 J. Rothe, M. A. Denecke, K. Dardenne and T. Fanghänel, The INE-Beamline for actinide research at ANKA, *Radiochim. Acta*, 2006, **94**(9–11), 691–696.
- 41 G. N. George and I. J. Pickering, *EXAFSPAK: A suite of computer programs for analysis of X-ray absorption spectra*, SSRL, Stanford, 1995.
- 42 M. Newville, IFEFFIT: interactive XAFS analysis and FEFF fitting, *J. Synchrotron Radiat.*, 2001, **8**(2), 322–324.
- 43 B. Ravel and M. Newville, ATHENA, ARTEMIS, HEPHAESTUS: data analysis for X-ray absorption spectroscopy using IFEFFIT, *J. Synchrotron Radiat.*, 2005, **12**(Pt 4), 537–541.
- 44 A. L. Ankudinov, B. Ravel, J. J. Rehr and S. D. Conradson, Real-space multiple-scattering calculation and interpretation of X-ray-absorption near-edge structure, *Phys. Rev. B: Condens. Matter Mater. Phys.*, 1998, **58**(12), 7565–7576.
- 45 J. J. Rehr, J. J. Kas, M. P. Prange, A. P. Sorini, Y. Takimoto and F. Vila, Ab initio theory and calculations of X-ray spectra, *C. R. Phys.*, 2009, **10**(6), 548–559.
- 46 Z. V. Akhmerkina, L. B. Serezhkina, V. N. Serezhkin, Y. N. Mikhajlov and Y. E. Gorbunova, Crystal structure of Ba[UO₂(C₂O₄)₂(H₂O)]·4H₂O, *Zhurnal Neorganicheskoy Khimii*, 2004, **49**(10), 1692–1695.
- 47 F. Furche, R. Ahlrichs, C. Hättig, W. Klopper, M. Sierka and F. Weigend, Turbomole, *Wiley Interdiscip. Rev.: Comput. Mol. Sci.*, 2014, **4**(2), 91–100.
- 48 A. D. Becke, A new mixing of Hartree-Fock and local density-functional theories, *J. Chem. Phys.*, 1993, **98**(2), 1372.
- 49 W. Küchle, M. Dolg, H. Stoll and H. Preuss, Energy-adjusted pseudopotentials for the actinides. Parameter sets and test calculations for thorium and thorium monoxide, *J. Chem. Phys.*, 1994, **100**(10), 7535.
- 50 F. Weigend and M. Häser, RI-MP2: first derivatives and global consistency, *Theor. Chem. Acc.*, 1997, **97**(1–4), 331–340.
- 51 F. Weigend, M. Häser, H. Patzelt and R. Ahlrichs, RI-MP2: optimized auxiliary basis sets and demonstration of efficiency, *Chem. Phys. Lett.*, 1998, **294**(1–3), 143–152.
- 52 A. Klamt and G. Schüürmann, COSMO: a new approach to dielectric screening in solvents with explicit expressions for the screening energy and its gradient, *J. Chem. Soc., Perkin Trans. 2*, 1993, (5), 799.
- 53 A. Skerencak, P. J. Panak, W. Hauser, V. Neck, R. Klenze, P. Lindqvist-Reis and T. Fanghanel, TRILFS study on the complexation of Cm(III) with nitrate in the temperature

- range from 5 to 200 degrees C, *Radiochim. Acta*, 2009, **97**(8), 385–393.
- 54 C. Reichardt, Solvatochromic Dyes as Solvent Polarity Indicators, *Chem. Rev.*, 1994, **94**(8), 2319–2358.
 - 55 V. Neck, T. Fanghänel, G. Rudolph and J. I. Kim, Thermodynamics of Neptunium(V) in Concentrated Salt Solutions: Chloride Complexation and Ion Interaction (Pitzer) Parameters for the NpO_2^+ Ion, *Radiochim. Acta*, 1995, **69**(1), 39–47.
 - 56 M. W. Cooper, M. J. Rushton and R. W. Grimes, A many-body potential approach to modelling the thermomechanical properties of actinide oxides, *J. Phys.: Condens. Matter*, 2014, **26**(10), 105401.
 - 57 M. Takano, M. Akabori, Y. Arai and K. Minato, Thermal expansion of TRU nitride solid solutions as fuel materials for transmutation of minor actinides, *J. Nucl. Mater.*, 2009, **389**(1), 89–92.
 - 58 H. Serizawa, Y. Arai, M. Takano and Y. Suzuki, X-ray Debye temperature and Grüneisen constant of NpO_2 , *J. Alloys Compd.*, 1999, **282**(1–2), 17–22.
 - 59 M. Uematsu and E. U. Frank, Static Dielectric Constant of Water and Steam, *J. Phys. Chem. Ref. Data*, 1980, **9**(4), 1291–1306.
 - 60 J. B. Hasted, D. M. Ritson and C. H. Collie, Dielectric Properties of Aqueous Ionic Solutions. Parts I and II, *J. Chem. Phys.*, 1948, **16**(1), 1–21.
 - 61 Z. Zhang, Y. Yang, G. Liu, S. Luo and L. Rao, Effect of temperature on the thermodynamic and spectroscopic properties of $\text{Np}(\text{v})$ complexes with picolinate, *RSC Adv.*, 2015, **5**(92), 75483–75490.
 - 62 Y. Yang, Z. Zhang, G. Liu, S. Luo and L. Rao, Effect of temperature on the complexation of NpO_2^+ with benzoic acid: Spectrophotometric and calorimetric studies, *J. Chem. Thermodyn.*, 2015, **80**, 73–78.
 - 63 P. G. Daniele, C. Rigano and S. Sammartano, The formation of proton and alkali-metal complexes with ligands of biological interest in aqueous solution. Thermodynamics of HS^+ , Na^+ and K^+ – oxalate complexes, *Thermochim. Acta*, 1981, **46**, 103–116.
 - 64 P. G. Daniele, C. Rigano and S. Sammartano, The formation of proton and alkali metal complexes with ligands of biological interest in aqueous solution. Thermodynamics of HS^+ , Na^+ and K^+ – dicarboxylate complex formation, *Thermochim. Acta*, 1983, **62**, 101–112.
 - 65 R. M. Kettler, D. A. Palmer and D. J. Wesolowski, Dissociation quotients of oxalic acid in aqueous sodium chloride media to 175 °C, *J. Solution Chem.*, 1991, **20**(9), 905–927.
 - 66 L. Alderighi, P. Gans, A. Ienco, D. Peters, A. Sabatini and A. Vacca, Hyperquad simulation and speciation (HySS): a utility program for the investigation of equilibria involving soluble and partially soluble species, *Coord. Chem. Rev.*, 1999, **184**(1), 311–318.
 - 67 I. Puigdomènech, J. A. Rard, A. V. Plyasunov, I. Grenthe, L. Seine-st Germain and B. Des Îles, *Temperature corrections to thermodynamic data and enthalpy calculations*, Le Seine-St. Germain 12, Bd. des Îles, F-92130 Issy-les-Moulineaux, France, 1999.
 - 68 W. Hummel, I. Puigdomènech, L. Rao and O. Tochiyama, Thermodynamic data of compounds and complexes of U, Np, Pu and Am with selected organic ligands, *C. R. Chim.*, 2007, **10**, 948–958.
 - 69 M. M. Maiwald, T. Sittel, D. Fellhauer, A. Skerencak-Frech and P. J. Panak, Thermodynamics of neptunium(v) complexation with sulfate in aqueous solution, *J. Chem. Thermodyn.*, 2018, **116**, 309–315.
 - 70 M. M. Maiwald, D. Fellhauer, A. Skerencak-Frech and P. J. Panak, The complexation of neptunium(v) with fluoride at elevated temperatures: Speciation and thermodynamics, *Appl. Geochem.*, 2019, **104**, 10–18.
 - 71 M. M. Maiwald, A. Skerencak-Frech and P. J. Panak, The complexation and thermodynamics of neptunium(v) with acetate in aqueous solution, *New J. Chem.*, 2018, **42**(10), 7796–7802.
 - 72 R. J. Motekaitis, A. E. Martell and R. M. Smith, *NIST Critically Selected Stability Constants of Metal Complexes. NIST Standard Reference Database 46, version 6*, U.S. Department of Commerce, Technology Administration, National Institute of Standards and Technology, Standard Reference Data Program, Gaithersburg, MD, 2001.
 - 73 A. Skerencak-Frech, M. Maiwald, M. Trumm, D. R. Fröhlich and P. J. Panak, The complexation of $\text{Cm}(\text{III})$ with oxalate in aqueous solution at $T = 20\text{--}90$ degrees C: a combined TRLFS and quantum chemical study, *Inorg. Chem.*, 2015, **54**(4), 1860–1868.
 - 74 D. R. Fröhlich, A. Skerencak-Frech and P. J. Panak, A spectroscopic study on the formation of $\text{Cm}(\text{III})$ acetate complexes at elevated temperatures, *Dalton Trans.*, 2014, **43**(10), 3958–3965.
 - 75 M. M. Maiwald, K. Dardenne, J. Rothe, A. Skerencak-Frech and P. J. Panak, Thermodynamics and Structure of Neptunium(v) Complexes with Formate. Spectroscopic and Theoretical Study, *Inorg. Chem.*, 2020, **59**(9), 6067–6077.
 - 76 K. Takao, S. Takao, A. C. Scheinost, G. Bernhard and C. Hennig, Complex formation and molecular structure of neptunyl(VI) and -(V) acetates, *Inorg. Chem.*, 2009, **48**(18), 8803–8810.
 - 77 P. G. Allen, J. J. Bucher, D. K. Shuh, N. M. Edelstein and T. Reich, Investigation of Aquo and Chloro Complexes of UO_2^{2+} , NpO_2^+ , Np^{4+} , and Pu^{3+} by X-ray Absorption Fine Structure Spectroscopy, *Inorg. Chem.*, 1997, **36**(21), 4676–4683.
 - 78 T. Reich, G. Bernhard, G. Geipel, H. Funke, C. Hennig, A. Roßberg, W. Matz, N. Schell and H. Nitsche, The Rossendorf Beam Line ROBL – a dedicated experimental station for XAFS measurements of actinides and other radionuclides, *Radiochim. Acta*, 2000, **88**(9–11), 633–638.
 - 79 R. D. Hancock and A. E. Martell, The Chelate, Cryptate and Macrocyclic Effects, *Comments Inorg. Chem.*, 1988, **6**(5–6), 237–284.

Repository KITopen

Dies ist ein Postprint/begutachtetes Manuskript.

Empfohlene Zitierung:

Maiwald, M. M.; Trumm, M.; Dardenne, K.; Rothe, J.; Skerencak-Frech, A.; Panak, P. J.
[Speciation, thermodynamics and structure of Np\(V\) oxalate complexes in aqueous solution](#)
2020. Dalton transactions, 49
[doi: 10.554/IR/1000124323](#)

Zitierung der Originalveröffentlichung:

Maiwald, M. M.; Trumm, M.; Dardenne, K.; Rothe, J.; Skerencak-Frech, A.; Panak, P. J.
[Speciation, thermodynamics and structure of Np\(V\) oxalate complexes in aqueous solution](#)
2020. Dalton transactions, 49, 13359–13371.
[doi:10.1039/d0dt02379e](#)

Lizenzinformationen: [KITopen-Lizenz](#)